PROGRESS IN COLOR, COLORANTS AND COATINGS

available online @ www.pccc.icrc.ac.ir

Prog. Color Colorants Coat. 5(2012), 91-99

Ministry of Science, Research and Technology
Institute for Color Science and Technology

A Comparison Study on Corrosion Behavior of Zinc Phosphate and Potassium Zinc Phosphate Anticorrosive Pigments

E. Alibakhshi[1], E. Ghasemi[2]*and M. Mahdavian[3]

[1.] M. Sc., Department of Surface Coating, Institute for Color Science and Technology, P. O. Box: 16765-654, Tehran, Iran.

[2.] Assistant Professor, Department of Inorganic Pigment and Glazes, Institute for Color Science and Technology, P. O. Box: 16765-654, Tehran, Iran.

[3.] Assistant Professor, (a) Department of Polymer Engineering and (b) Institute of Polymeric Materials, Sahand University of Technology, P. O. Box: 51335-19962, Tabriz, Iran.

ARTICLE INFO

Article history:
Received: 11-06-2012
Final Revised: 13-08-2012
Accepted: 14-08-2012
Available online: 15-08-2012

Keywords:
Corrosion inhibition
Pigment
Characterize
EIS
SEM-EDX
Raman.

ABSTRACT

In this article, the effect of potassium on the phase formation and anticorrosion properties of zinc phosphate pigments has been investigated. The co-precipitation method was selected as synthesis method of potassium zinc phosphate pigment. Then the synthesized pigment was characterized by x-ray diffraction (XRD), Fourier transform infrared (FTIR) and Raman spectroscopy. Morphology of the powders was investigated with scanning electron microscopy (SEM). The inhibition efficiency of this pigment was compared to the commercial zinc phosphate pigment in a 3.5 % NaCl solution by means of electrochemical impedance spectroscopy (EIS) on mild steel specimens. The surface composition and morphology of mild steel specimens after exposure to the test solutions were examined by scanning electron microscopy- energy dispersive X-ray spectroscopy (SEM-EDX). The results indicate the better corrosion inhibitive performance of potassium zinc phosphate in comparison with the commercial zinc phosphate. Prog. Color Colorants Coat. 5(2012), 91-99. © Institute for Color Science and Technology.

1. Introduction

Combination of zinc and phosphate which would be zinc phosphate (ZP) is the most important group of phosphate pigments. ZP pigment is a nontoxic compound with the following formulation:

$Zn_3(PO_4)_2.xH_2O$ (x=2 or 4)

The initial and the simplest generation of phosphate pigments were produced by mixing of disodium phosphate and zinc sulfate solution in boiling point. This method creates first generation of phosphate pigments which is ZP [1]. Inappropriate corrosion inhibition activity is the result of low solubility of this generation [2]. A small amount of phosphate can be released by ZP pigments, which is not enough to protect the metal

*Corresponding author: eghasemi@icrc.ac.ir

surface [3].

Second generation is created by modification of the cationic or anionic parts or the first generation [4-5]. The most important feature of this generation is the increased solubility in water. Aluminum zinc phosphate and molybedate zinc phosphate are of the most important pigments of this generation. Many studies have investigated the role of pigments of this generation in cathodic delamination of water base coatings [6-7].

There are different ways to study the inhibitive properties of such pigments. One of the most common methods is to study the corrosion of the bare metal immersed in extract solution of pigments [8]. Evaluation of the inhibitive effects in extract solutions could be useful in understanding the mechanism by which the anticorrosion pigments perform in the protective coatings.

Previously, Wei et al. [9] described the electrochemical behavior of potassium zinc phosphate ($KZn_2PO_4(HPO_4)$) in extract solution and coating. They found that this compound is a new engineered anticorrosive pigment because it can efficiently enhance the inhibition properties on cathodic delamination. Comparing with zinc phosphate, its solubility is enhanced which can be the reason of its higher inhibition efficiency.

In this article, we have synthesized and characterized the potassium zinc phosphate (PZP), and its inhibition performance was compared with commercial ZP by EIS and surface analysis method. The main difference between this work and the above mentioned work [9] is that in the published work, $KZn_2PO_4(HPO_4)$ is used while in our work PZP with all phases included in the final deposition is compared to ZP.

2. Experimental

2.1. Materials

Zinc chloride, phosphoric acid (85%), potassium hydroxide and triethanolamine were obtained from Merck and ZP pigment from Nubiola.

2.2. Pigments preparation

Zinc chloride (8.1 g) was added to a phosphoric acid solution (which was prepared by solving 6.2 ml of H_3PO_4 in 100 ml of water) and stirred with a magnetic stirrer to achieve a complete dissolution. Then 3.5 ml of triethanolamine were added and the solution further stirred for 15 min. Another solution prepared with solving of 4.2 g of KOH in 80 ml of deionized water and was added to the above mentioned solution and stirred 3 h, and heated at 100 °C for 24 h. The precipitate was recovered by filtration, washed to neutral pH and dried at 100 °C.

2. 3. Characterization of the pigments

The X-ray diffraction (XRD) was performed on as prepared PZP powder using Philips X-ray spectrometer, PW 1800 type (Netherlands) with Cu-kα filament. FTIR analysis was carried out using KBr disks in the region of 4000-400 cm^{-1} by using FTIR Perkin Elmer Spectrum One. Raman test was performed using Almega Thermo Nicolet Dispersive Raman Spectrometer on the prepared samples. The size and the shapes of the particles of synthesized PZP were studied by the LEO 1455VP (Angstrom Scientific Inc., USA) scanning electron microscope (SEM).

2. 4. Evaluation of the inhibitive properties of the pigments extracts

2.4.1. Sample preparation for electrochemical impedance spectroscopy (EIS) measurements

In order to run the EIS measurements, steel samples with the mentioned compositions of Table 1 were cut down into the pieces with 1 cm^2 surface area. On the following, a braided wire was attached to one side of steel pieces by brazing, then the steel samples were mounted by unsaturated polyester. Later, the mounted samples were abraded using emery paper 600 and 800. Finally, the samples were washed using methanol to remove any remaining contamination.

Elements	wt%
Fe	97.7
C	0.19
Si	0.415
Mn	1.39
P	<0.005
S	<0.005
Cr	0.026
Mo	0.018
Co	0.0559
Cu	0.0429

Table 1: The composition of the mild steel panels.

In order to prepare the test solutions, 1 g of each pigment was stirred in 1 liter of 3.5% w/w NaCl aqueous solution for 24 h and filtered. A blank solution of 3.5% NaCl containing no pigment was also prepared to take into account as a reference solution. Then steel samples were immersed in the test solutions for 24 h.

2.4.2. EIS

EIS measurements were carried out employing Ivium Compactstat (Netherlands) in the three electrode cell containing Ag/AgCl as a reference electrode, graphite as a counter electrodes from and steel samples as working electrode. EIS measurements implemented at OCP potential using 10mv perturbation in a frequency range of 10 kHz-10 mHz. Obtained data was analyzed using Iviumsoft software.

2.4.3. SEM-EDX

SEM-EDX test was implemented on mild steel panels with dimensions of 1 cm ×1 cm and thickness of 2 mm using Philips (XL30) after 24 h immersion in 100 mL test solutions. Afterwards, the samples were washed with distilled water and dried.

3. Results and discussions

3.1. Characterization of the synthesized pigment

3.1.1. X-ray powder diffraction

Figure 1 displays the XRD result for as synthesized pigment powders. Two forms of PZP including $KZnPO_4$ and $KZn_2PO_4.HPO_4$ can be detected as the major phases and ZnO as the minor phase. According to the relative intensity of the diffraction peaks, it can be concluded that the $KZn_2PO_4(HPO_4)$ is the major phase in the synthesized powder.

3.1.2. FTIR

Figure 2 shows the FTIR spectrum of the synthesized PZP powder. The absorption bands which are observed at 3160.8-3429 cm^{-1} is characteristic of the O-H stretching vibrations of free and hydrogen bonded surface hydroxyl groups [10]. A second typical absorption band at1559.29 and 1617.92cm^{-1} is assigned to physically adsorbed water (H-O-H bending) [11]. Absorption bands at 712.42 cm^{-1}, 781.95 cm^{-1} and 781.95 cm^{-1} belongs to P-O bending and stretched vibration [12]. The bands between 1211.86 - 1488.42 cm^{-1} show stretched vibration of P=O [13]. The bands associated with the ν_{OH} stretching frequencies of P-O-H appear at 2937.99 and 3080.94 cm^{-1} [14].

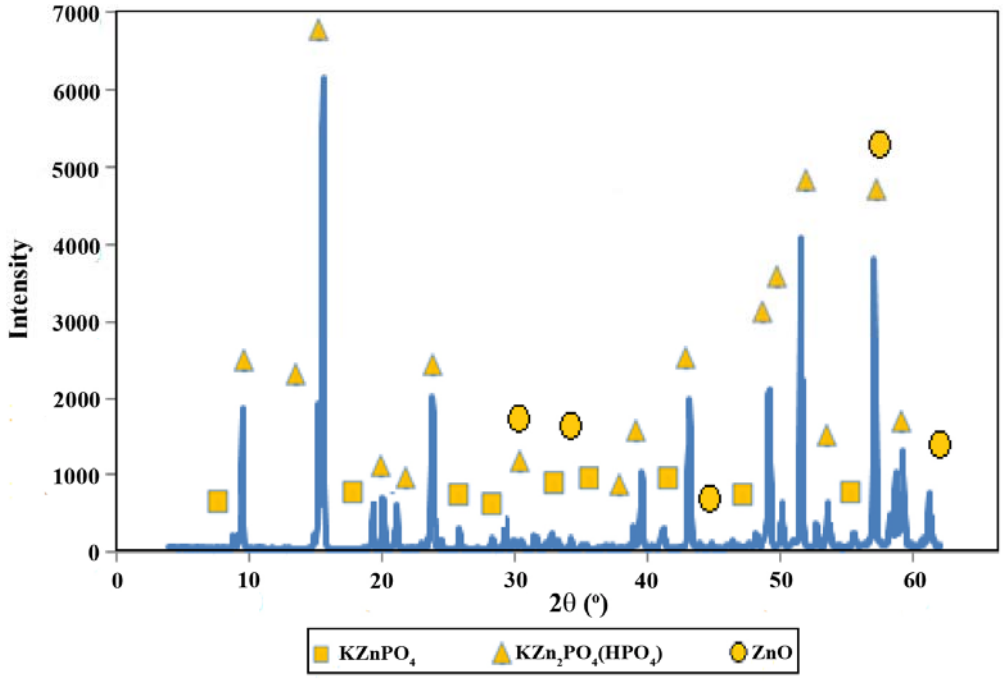

Figure 1: XRD pattern of as synthesized PZP sample.

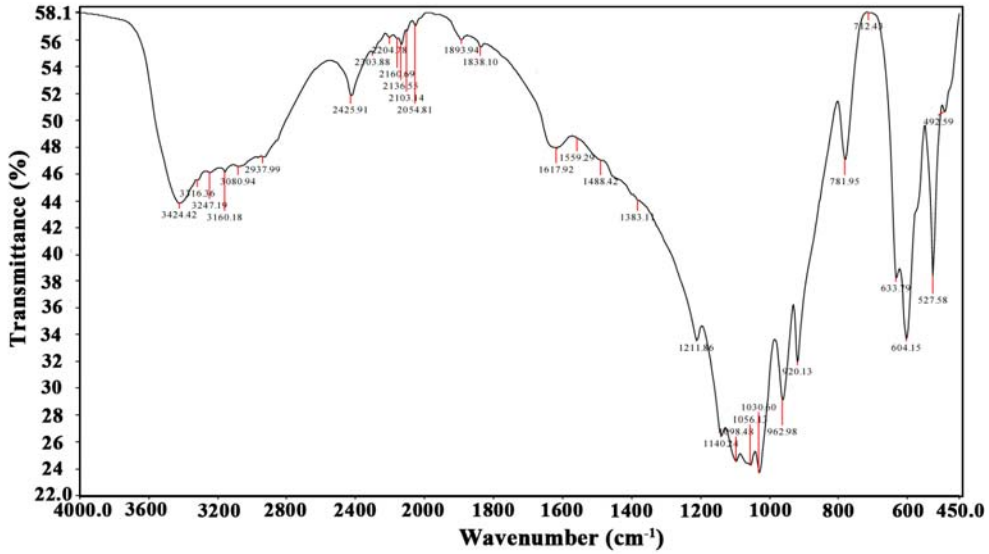

Figure 2: FTIR spectrum of the synthesized PZP.

The characteristic absorption bands of ZnO are observed at 1838.1-2425.91 cm^{-1} and 527.58-673.79 cm^{-1} [14]. Also, for K-O only an absorption band with a wave number of 492.59 cm^{-1} is observed. The bands at 962.98-1140.24 cm^{-1} are indications of Zn-O-P vibrations [15-16]. The above observed bands confirm the presence of $KZnPO_4$ and $KZn_2PO_4.HPO_4$ and ZnO phases, which are in accordance with XRD result.

3.1.3. Raman

The PZP phase was identified by Raman spectroscopic analysis. The Raman spectra and the characteristic bands of PZP are shown in Figure 3 and Table 2, respectively. The detected K-O, Zn-O, POP, PO_2 and PO_3 bands specifies the presence of K, Zn, O and P elements which can be related to the above mentioned phases. This reveals that the synthesized pigment has no unwanted impurity.

Table 2. Raman wave numbers and assignments of the prepared PZP.

Wave number (cm^{-1})	Assignments[17-20]
303	K-O, δ_{PO2}
490	Zn-O,δ_{PO2}
590	δ_{PO2}
766	ν_{POP} (sym)
910	ν_{POP} (asym)
1013-1074	ν_{PO3} (sym)
1137-1332	ν_{PO3} (asym)
1813-3429	OH

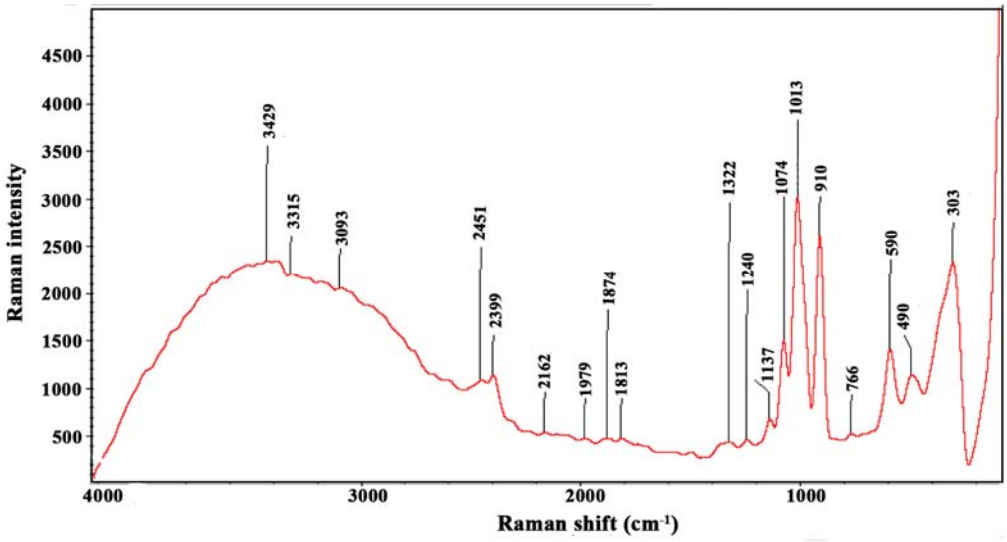

Figure 3: Raman spectrum of the synthesized PZP.

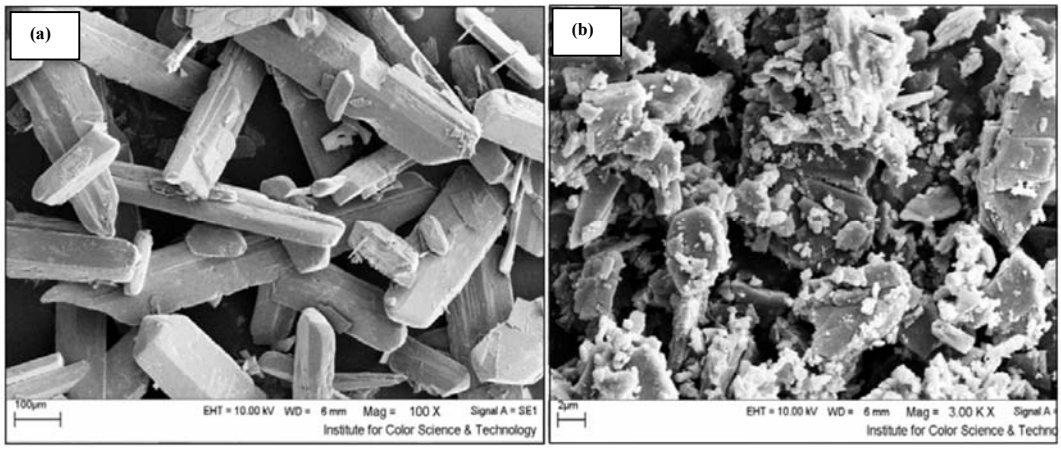

Figure 4: SEM micrograph of (a) PZP and (b) ZP.

3.2. Morphology of the synthesized pigment

The SEM micrographs of as prepared PZP and commercial ZP powders can be seen in Figure 4 It is clear that the morphologies of two samples are different. The PZP particles are rod-like which have been grown to several hundred micrometers, while ZP powders don't have uniform shape and are smaller in size compared to PZP powders.

3.3. Evaluation of the inhibitive properties of the pigments extracts

3.3.1. EIS

Figure 5 displays typical Bode (a) and Nyquist (b) diagrams of the mild steel specimens after 24h immersion in the 3.5% NaCl solution containing no pigment (blank) and ZP and PZP extracts in 3.5% NaCl solution. According to the diagrams, the presence of PZP

in sodium chloride solution can increase the impedance at low frequencies to the higher amounts, comparing to the ZP extract and blank solution. Also, only one relaxation time could be observed for the mild steel samples immersed in ZP extracts showing that it could only influence the charge transfer process. The presence of second relaxation time in the PZP extract indicates the formation of a protective film at the mild steel surface.

Figure 6 shows equivalent circuits to fit the EIS results, where R_s represents solution resistance, R_{ct} charge transfer resistance, CPE_{dl} the constant phase element of the double layer, R_f protective film resistance and CPE_f constant phase element of protective film.

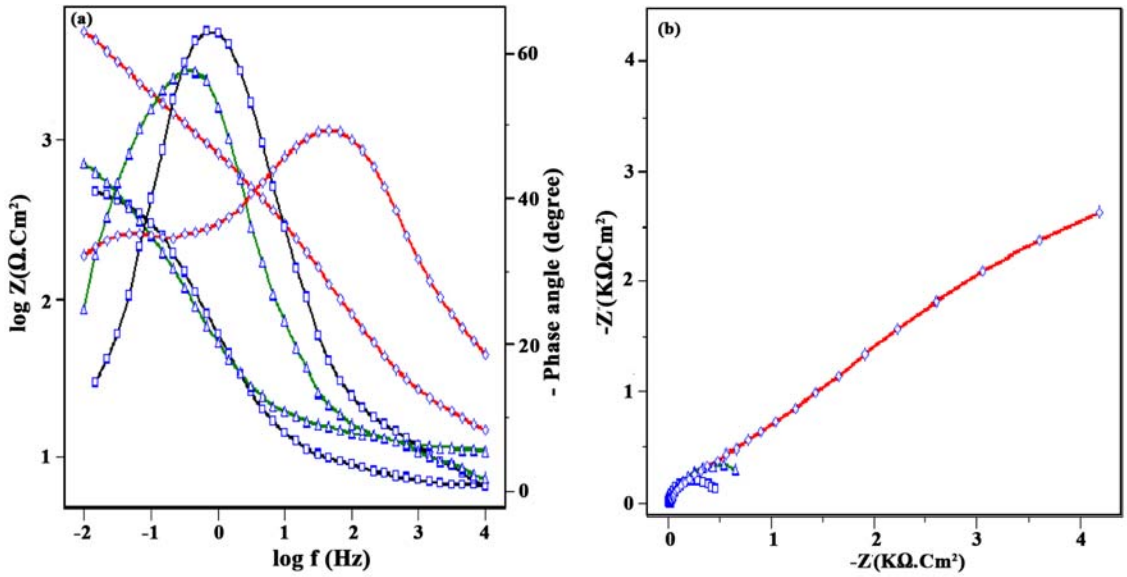

Figure 5: The diagrams of (a) Bode and (b) Nyquist for mild steel samples after 24 h of immersion in 3.5% NaCl solution containing no pigmented (□), ZP (Δ) and PZP (◊).

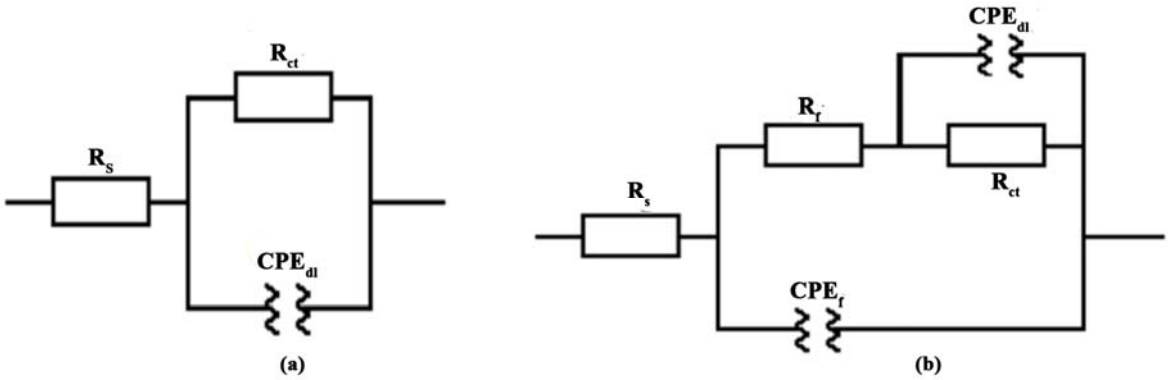

Figure 6: Equivalent electrical circuit with (a) one time constant and (b) two time constant.

The double layer and protective film capacitance values could be calculated by the Eq. 1 [21, 22].

$$C = (Y_0.R^{1-n})^{\frac{1}{n}} \quad (1)$$

where, Y_0 is the magnitude of admittance of the CPE (in $S^n.\Omega^{-1}.\ cm^{-2}$) and n is the CPE exponent, as $n = \alpha/(\pi/2)$ (α is the constant phase angle of the CPE). The n value has a meaning of phase shift and can characterize different surface phenomena such as surface heterogeneity resulting from surface roughness, dissolution of the metal, impurities, and distribution of the active sites, inhibitor adsorption and porous layer formation.

Extracted electrochemical parameters obtained from fitted EIS results are listed in Table 2. It can be seen that the presence of potassium in ZP structure leads to charge transfer resistance increment of saturated solution. The capacitance and admittance value of samples immersed in PZP extract is lower than those immersed in ZP extract and blank solution. $Y_{0,dl}$ for PZP is less than ZP, which in physical terms can be either associated with the formation of a compact dielectric film or it may correspond to the increase of the electrical double layer thickness. The n_{dl} value of mild steel immersed in blank solution is higher than the one immersed in 3.5% NaCl solutions containing ZP and PZP.

3.3.2. SEM-EDX

EDX determines the chemical composition of the corrosion products formed at the surface. This elemental composition of the surface layer shown in Table 3 indicates that the mild steel specimens are covered by some species of ZP and PZP.

Considering the precision of EDX analysis, there are only small amount of Na (atomic weight: 23 g/mol) and Cl (atomic weight: 35.5 g/mol) on the mild steel immersed in the blank solution however, in the case of ZP and PZP there is no Na and Cl on the surface indicating that the complex layer formed on the surface are neutral.

Table 3: Electrochemical parameters of the mild steel after 24 h exposure to blank solution and ZP and PZP extracts.

Pigment	R_{ct} ($\Omega.cm^2$)	$Y_{0,dl}$ ($\mu s^n.\Omega^{-1}.cm^{-2}$)	n_{dl}	C_{dl}($\mu F/cm^2$)	R_f ($\Omega.cm^2$)	$Y_{0,f}$ ($\mu s^n.\Omega^{-1}.cm^{-2}$)	n_f	C_f($\mu F/cm^2$)
Blank	529±28.2	544.5±362	0.64	270.35	-	-	-	-
ZP	755.6±59.1	25.59±9	0.53	1.93	-	-	-	-
PZP	9016.5±1751	1.64±0.9	0.54	0.04	950.5±372.1	2.6±1.9	0.63	0.07

Table 4: EDX result (wt %) of steel samples immersed for 24 h in blank solution and ZP and PZP extracts.

	Fe	Zn	P	Na	Cl	K
Blank solution	balance	0	0	0.18	0.17	0
ZP Extract	balance	1.51	0.32	0	0	0
PZP Extract	balance	1.2	0.15	0	0	0.22

Although in the previous research [9] the higher inhibition effect of PZP is related to its higher solubility in water, their effect on surface films could be also influential. In the presence of ZP and PZP, there is a considerable amount of Zn and P on the surface, which could be related to the formation of protective layer composed of $Zn(OH)_2$ and $Fe_3(PO_4)$. The presence of K on the mild steel surface exposed to PZP extract indicates that there is a chance for deposition of PZP on the surface, which could be responsible for better protective performance of PZP compared to ZP. Figure 7 depicts the morphology of the mild steel after 24 h exposure in the 3.5% NaCl solution containing no pigment (a), ZP (b) and PZP (c) extracts.

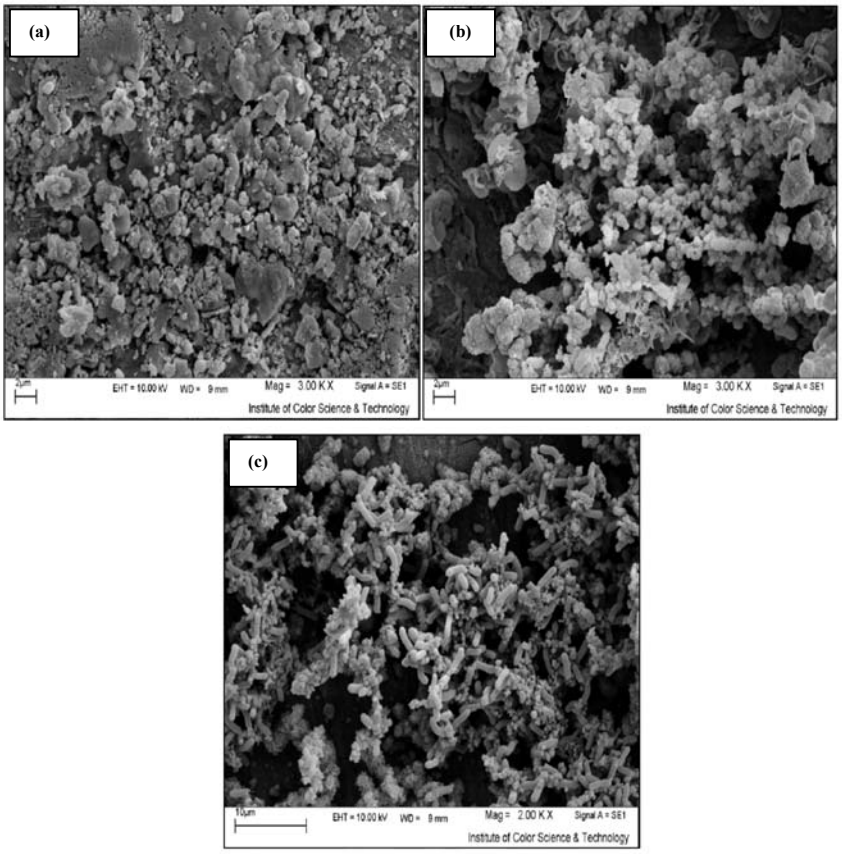

Figure 7: SEM micrograph of the mild steel samples after 24 h immersion in 3.5% NaCl solution containing (a) no pigment, (b) ZP and (c) PZP.

4. Conclusions

The PZP pigment was synthesized successively via co-precipitation method. The results of XRD, FTIR and Raman techniques exhibited same results which confirmed that the synthesized pigment contains KZn_2PO_4 (HPO_4), $KZnPO_4$, and ZnO as major to minor phases, respectively, with no other impurities. From the SEM studies it was depicted that the particles of PZP have extra grown rod-like morphologies. Inhibitive performance of PZP was compared with commercial ZP by EIS and EDX. According to the EIS results, the modified pigment (PZP) revealed greater inhibitive properties compared to the conventional ZP pigment.

Acknowledgements

The authors would like to thank National Iranian Drilling Company (NIDC) for financial supports.

5. References

1. A. Z. Gomaa, H. A. Gad, Some anticorrosive primers free of lead and chromate, JOCCA., 71(1988), 51-55.
2. M. Svoboda, The influence of soluble sulfates on the inhibitive capacity of zinc phosphate, Ferbe Lack., 92(1988), 701-703.
3. C. Robu, N. Orban, G. Varga, Anticorrosive lead free pigments combination, *Polym., Paint Color J.,* 177(1987), 566-569.
4. A. Gerhard, A. Bittner, Second generation phosphate anti-corrosive pigments. formulating rules for full replacement of new anti-corrosive pigments, *J. Coat. Technol.,* 58(1986), 59-65.
5. B. Del-Amo, R. Romagnoli, V. F. Vetere, Steel corrosion protection by means of alkyd paints pigmented with calcium acid phosphate, *Ind. Eng. Chem. Res.,* 38(1999), 2310-2314.
6. H. Leidheiser, W. Wang, L. Igetoft, The mechanism for cathodic delamination of organic coatings from a metal surface, *Prog. Org. Coat.,* 11(1983), 19-41.
7. L. S. Hernandez, B. Del-Amo, R. Romagnoli, Accelerated and EIS tests for anticorrosive paints pigmented with ecological pigments, *Anti-Corros. Methods Mater.,* 46(1999), 194-204.
8. M. Mahdavian, M. Attar, Evaluation of zinc phosphate and zinc chromate effectiveness via AC and DC methods, *Prog. Org. Coat.,* 53(2005), 191-194.
9. D. Wei, S. Ma, Z. Zhou, Z. Huang, A. Yuan, A. Liao, Electrochemical behavior of potassium zinc phosphates extract and coating, *Appl. Mech. Mater.,* 152(2012), 64-67.
10. R. Wang, K. Hashimoto, A. Fujishima, M. Chikuni, E. A. Kojima, A. Kitamura, M. Shimohi-goshi, T. Watanabe, Photogeneration of highly amphiphilic TiO_2 surfaces, *Adv. Mater.,* 10(1998), 135-138.
11. D. Dvoranova, V. Brezova, M. Mazura, M. A. Malati, Investigations of metal-doped titanium dioxide photocatalysts, *Appl. Catal., B,* 37(2002), 91-105.
12. H. Rathore, G. Varshney, S. Mojumdar, M. Saleh, Synthesis, characterization and fungicidal activity of zinc diethyldithiocabamate and phosphate, *J. Therm. Anal. Calorim.,* 3(2007), 681-686.
13. G. Goplakrishna, S. Madhu, M. Mahendra, B. Doreswamy, M. Mahesh, M. Sridhar, J. Shashidhara, Hydrothermal synthesis, crystal structure and characterization of $2(LiZnHP_2O_7)$, *Mater. Lett.,* 60(2006), 613-617.
14. D. Chen, Sh. Ma, H. Yu, A. Yuan, A. Liao, J. Wu, Thermal decomposition kinetic and electrochemical properties of $KZn_2(PO_4)(HPO_4)$, *Adv. Mater. Res.,* 152(2011), 184-191.
15. O. Pawlig, R. Trettin, In-situ DRIFT spectroscopic investigation on the chemical evolution of zinc phosphate acid-base cement, *Chem. Mater.,* 12(2000), 1279-1287.
16. D. Sun, J. Deng , Z. Chao, Catalysis over zinc-incorporated berlinite ($ZnAlPO_4$) of the methoxycarbonylation of 1,6-hexanediamine with dimethyl carbonate to form dimethylhexane-1,6-dicarbamate, *Chem. Cent. J.,* 1(2007), 1-27.
17. O. Pawlig, V. Schellenschlager, H. D. Lutz, R. Trettin, Vibrational analysis of iron and zinc phosphate conversion coating constituents, *Spectrochim. Acta, Part A,* 57(2001), 581-590.
18. M. Hernandez, J. Genesca, J. Uruchurtu, F. Galliano, D. Landolt, Effect of an inhibitive pigment zincaluminumphosphate (ZAP) on the corrosion mechanisms of steel in waterborne coatings, *Prog. Org. Coat.,* 56(2006), 199-206.
19. G. Stranford, R. Condrate, The raman spectrum of α-zinc pyrophosphate, *J. Mol. Struct.,* 73(1981), 231-234.
20. J. Wang, D. Li, J. Liu, X. Yang, J. He, Y. Lu, One-step preparation and characterization of zinc phosphate nanocrystals with modified surface, *Soft Nanosci. Lett.,* 1(2011), 81-85.
21. M. Mahdavian, M. M. Attar, Electrochemical behaviour of some transition metal acetylacetonate complexes as corrosion inhibitors for mild steel, *Corros. Sci.,* 51(2009), 409-414.
22. M. Motamedi, A. R. Tehrani-Bagha, M. Mahdavian, A comparative study on the electrochemical behavior of mild steel in sulfamic acid solution in the presence of monomeric and gemini surfactants, *Electrochim. Acta*, 58(2011), 488-496.